

Time-series analysis of GPS monitoring data from a long-span bridge considering the global deformation due to air temperature changes

Hien Van Le¹  · Mayuko Nishio¹

Received: 22 October 2014 / Revised: 21 May 2015 / Accepted: 21 May 2015 / Published online: 31 May 2015
© Springer-Verlag Berlin Heidelberg 2015

Abstract Although the structural health monitoring (SHM) based on the displacement measurement has been adopted in some cases of long-span bridges and recognized several advantages, there are some issues required to be considered, such as in acquiring the long-term static displacements with high and stable accuracies and in converting large amount of data into usable information. The global positioning system (GPS) is expected to solve those issues. This study aims to analyze the GPS time-series data acquired in a cable-stayed bridge in Vietnam, and to verify the usable feature for the structural condition assessment. Here, we suggest the use of the global deformations that are due to the periodic air temperature changes. Firstly, we observed the quality of acquired GPS data, and the missing data was interpolated by applying the least-squares estimation. The correlation coefficient analysis was then conducted using both the GPS and the air temperature data to understand the global deformation due to temperature changes. It was clarified that the global towers-girder coupled deformation was dominated by the 1-day periodic temperature change. The autoregressive integrated moving average (ARIMA) model was then applied to the GPS time-series data, and it was shown that there were high regressions in some AR-MA coefficients plots. It was thus concluded that those plots could be used as the base distributions for the statistical structural condition assessment.

Keywords Global positioning system · Long-span bridges · Time-series analysis · Global deformation · Temperature effects · ARIMA model

1 Introduction

Structural health monitoring (SHM) has been considered for the process of implementing structural condition assessment for civil infrastructures as well as for the large-scaled structures, such as long-span bridges. In those flexible bridges, some structural changes have been considered to relate closely to deformations [1]. A bridge usually has two kinds of individual deformations: long-term and short-term deformations. The long-term deformations are irrecoverable or periodic; they are caused by the foundation settlement, the creep, the temperature effects, and so on. The short-term deformations are caused by dynamic inputs, such as those induced by wind, tidal current, earthquake, and traffic [1–3]. The monitoring of those deformations is thus expected to be appropriate to capture the structural changes.

The SHM system have been applied to the continuous monitoring of civil structures; however, they still have some issues required to be considered, such as how to acquire the long-term static displacements of large-scale structures with stable and high accuracies, and how to convert large amount of data into usable information. In most cases of SHM, the major devices to capture dynamic/static structural responses are the accelerometer and the strain sensor; on the other hand, there are some sensors for measuring the structural displacements, such as the laser interferometer and some electronic distance instruments. Although those sensors have the advantage of high accuracies; they also have some disadvantages; e.g., it is

✉ Hien Van Le
hienlv84.uct@gmail.com; le-hien-my@ynu.jp

Mayuko Nishio
nishio@ynu.ac.jp

¹ Department of Civil Engineering, Yokohama National University, Yokohama, Japan

difficult to capture the measurement points when the displacement becomes too large, it is difficult to acquire data in real time, and the data acquisition is limited by climate conditions; i.e., the clear line of sight is one of basic requirements [4].

The Global Positioning System (GPS) technology has been successfully used to measure displacements of oscillating flexible civil engineering structures, such as suspension bridges and high-rise buildings. There are some advantages of the GPS technology to monitor the displacements of the large-scaled civil structures; e.g., it overcomes the limitation of climate, it can also measure the structural displacements in the three-dimensional directions at centimeter level accuracy [1, 4]. Actually, there are some cases of the SHM using GPS technology for the monitoring of long-span bridges; e.g., the Tianjin Yonghe cable stayed bridge in Hong Kong [2], the Akashi Kaikyo Bridge in Japan [5]. In the case of the Akashi Kaikyo Bridge which is a suspension bridge with the center span of 1991 m, the GPS system has been installed to measure the displacements in three directions at three locations; the center span, the top of one of towers and the anchorage. In the indicated study in [5], possibility to evaluate the configuration of a suspension bridge was shown based on the statistical methods that were applied to the acquired long-term GPS data. Here, the deformations due to an earthquake and the typhoon were identified.

On the other hand, some papers studied the continuous structural monitoring data, in most of which, the dynamic characteristics were used to verify the structural changes [6–8]. Those studies pointed out that the long-term monitoring data were greatly affected by the environmental and operational effects. Sohn et al. [6] mentioned that those effects consisted of temperature, humidity, and the changes in operational loads and boundary conditions. The variability of monitoring data due to the environmental effects could then mask more subtle structural changes caused by damages. In their study, a linear adaptive filter model was examined to discriminate the changes of modal parameters due to temperature changes from those caused by structural damage or other environmental effects. The results indicated that a linear adaptive filter to could reproduce the natural variability of the frequencies with respect to time of a day. Cornwell et al. [7] studied the variability in modal parameters due to the environmental effects and the operational conditions. In their study, the correlation analysis was conducted using the resonant frequencies and the temperature data measured in two data acquisitions, and the high correlation coefficients among them indicated the high influences of the temperature changes on the changes of structural properties. Farrar et al. [8] studied quantifying the variability in identified modal parameters caused by some sources, such

as variability in testing procedures, in test conditions, and the environmental variability. Most of those studies then concluded that the consideration of the variability in monitoring data due to the environmental and operational effects was a requirement for effective SHM.

There were then actually some studies that used the time-series analysis to assess the structural conditions from the monitoring data that consisted of the environmental and operational effects. Omenzetter et al. [9] used a seasonal autoregressive integrated moving average model with exogenous inputs (SARIMAX) and transfer function to model the relationship between strain data and temperature data. In this study, unusual structural condition changes or damages could be detected by applying the outlier detection and the intervention analysis technique to the estimated model. In the other study from the same authors [10], the approach to apply a vector seasonal autoregressive integrated moving average (ARIMA) time-series model was also presented. This study showed that the coefficients of the ARIMA model that were estimated by the adaptive Kalman filter could also be used for detecting the unusual events occurred on the structure. Additionally, the study by Sohn et al. [11] statistically examined the changes in the autoregressive (AR) model coefficients that estimated from dynamic data. It was shown that the distributions of AR coefficients estimated from data sets, which were from undamaged and damaged systems, could be appropriately classified to exact conditions.

This study aims to analyze the long-term displacement data acquired from a GPS monitoring system in a cable-stayed bridge. We investigated the global deformation patterns mainly due to the temperature effects, and verified whether they can be used as the structural response features for the statistical structural condition assessment. The target bridge here is the Can Tho bridge, which is a cable-stayed bridges in Vietnam. The quality of obtained GPS data is discussed and the missing data are handled by applying the least-square approximation to interpolate missing values. Then the correlation coefficient analysis is conducted using the GPS data and the air temperature data to investigate the global deformation modes due to the temperature effects. We then also verify the applicability of one of the time-series models; the ARIMA model for using the global deformations for the statistical structural condition assessment.

2 Time-series GPS data acquired in a target cable-stayed bridge

In general, the GPS system consists of the base stations, the rover stations, and the communication system. The selections of the reference stations and the remote stations are

very important to get good-quality data. In the case of long-span bridges monitoring, the distance between the base station and each of the rover stations is often set up to satisfy the effects of atmospheric and orbital errors are expected to be very small. However, the missing data are often occurred during the data acquisition due to some reasons, such as the problems in the communication system or in the data logger. Here, the target bridge in this study and the installed GPS system are firstly presented, and the handling of missing data in acquired data is also verified.

2.1 Target bridge and installed GPS system

The target bridge is the longest cable-stayed bridge in the South East Asia opened in 2010. Figure 1 shows the location and a picture of the target bridge. It is the bridge over the Hau river in the south of Vietnam, with the total length of 2750 m, the center span of 550 m, and the height of towers are 171 m. The bridge has a concrete box-girder with the width of 26 m; however, to increase the loading capacity, a part of the center span (middle 210 m length) is made by a steel box-girder. The girders constrained at the towers link to towers by using the elastic rubber bearings. There are two locations of elastic rubber bearings at the towers that are lateral bearings and vertical bearings. Thus, the girders are free to slide longitudinal at the limitation of bearings. The thermal expansion joints are located at the two ends of the main bridge. The SHM system has been installed since 2010, which includes not only the GPS system but also many sensors, such as temperature sensors, anemometers, and accelerometers.

The GPS system installed in the bridge consists of nine sensors as the rover stations and two base stations as shown in Fig. 2. The rover stations were placed on the top of two towers, the center span of the girder (the upstream and downstream sides), the quarter of the center span (the upstream and downstream sides), and on the top of piers. One of two base stations was placed on the footing of the North tower, while the other one was placed near the monitoring management office that was located 1-km far away from

the southern side of the bridge. The adopted GPS equipments were the products of Leica co., Ltd, GMX 902 GG model. The accuracies of the GPS system based on real time kinematic technique are ($\pm 10 \text{ mm} \pm 1 \text{ ppm}$) (part per million) for the horizontal plane and ($\pm 20 \text{ mm} \pm 1 \text{ ppm}$) for the vertical direction. The data acquisition system was constructed, in which the GPS signal at each rover station was acquired in 20 Hz, and their 10-min-averaged values were calculated. The averaged three-dimensional coordinates from the base station on the footing of the North tower were then acquired in each 10 min; therefore, the data became time-series data with 10-min interval. Figure 3a–c shows a part of raw GPS data at the center span acquired from February 15th to 22nd in 2013. Here, the x -direction in (a) is the longitudinal direction of the bridge, (b) is the y -direction that is in the lateral direction, and the z -direction in (c) is the vertical direction.

2.2 Handling of missing parts in GPS data

Actually, many small missing parts, most of which were less than five missing points, were observed in the raw GPS data. For handling those missing parts, a simple interpolation procedure was adopted for the time-series analysis. There were actually some previous studies that verified the handling methods of missing data [12, 13]; when a few data points are missing, it may be possible to interpolate the missing values by the polynomial function estimation on the basis of the least-square method [13]. Here, considering a polynomial function with m -th order:

$$y = a_0 + a_1t + a_2t^2 + \dots + a_mt^m. \tag{1}$$

Equation (1) can be rewritten by a matrix form as:

$$y = M.a \tag{2}$$

where: the components of y is GPS displacement data y_i ($i = 1 - n$) around the missing part at time t ; M is a matrix of size $n \times (m + 1)$ that consists of t_i and a is a vector of coefficients a_j ($j = 0 - m$). Hence, the coefficients of the polynomial can be estimated by:

Fig. 1 The target bridge. **a** The location of bridge. **b** The Can Tho cable stayed bridge



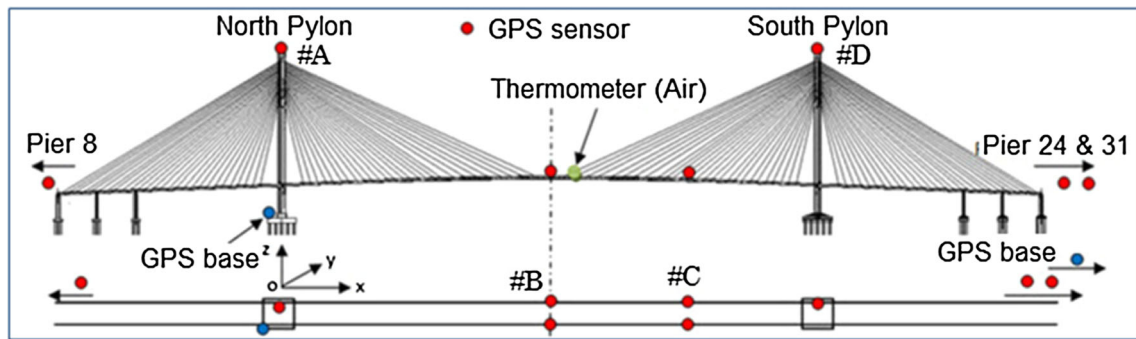


Fig. 2 GPS sensors on the Can Tho bridge

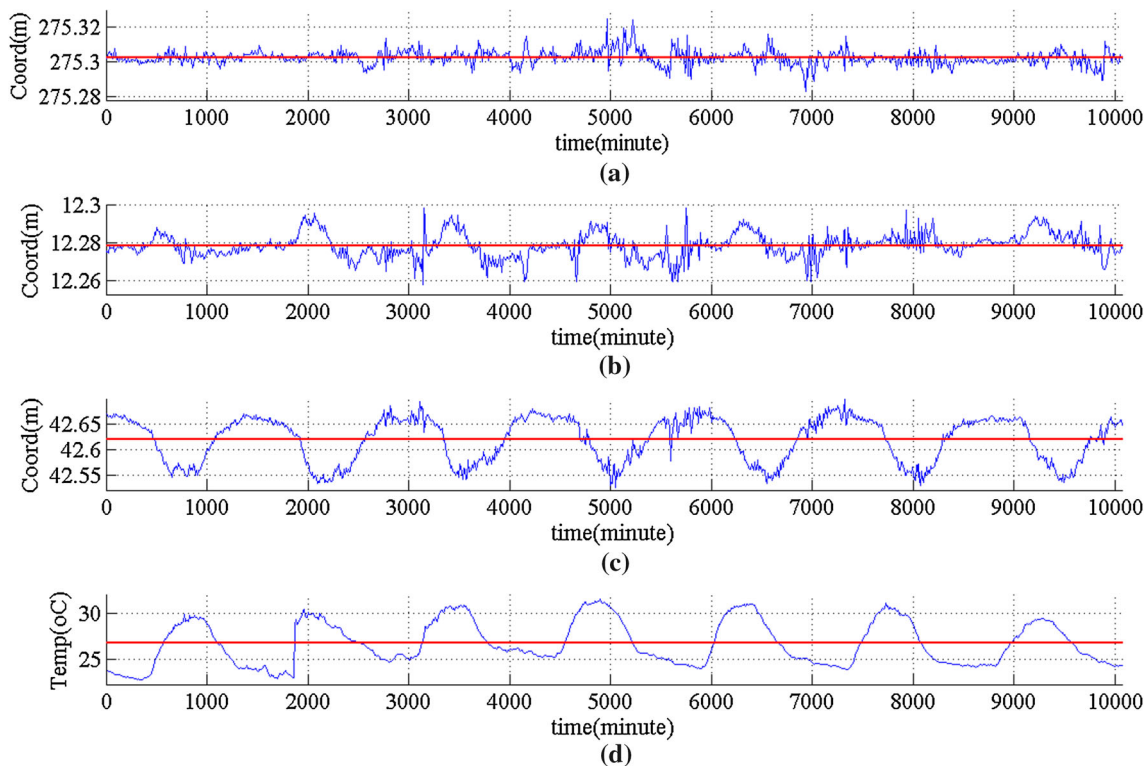


Fig. 3 Acquired time-series data by the installed GPS and temperature sensor (*blue line*: observed 1-week data, *red line*: the mean value of 1-week data). **a** *x*-direction, **b** *y*-direction, **c** *z*-direction, **d** temperature data

$$a = (M^T M)^{-1} M^T y. \quad (3)$$

Here, the order of the polynomial m must be determined; the accuracies of the interpolated points basically increase when the higher-order polynomials are used against the number of missing points.

The performance of interpolation was then verified for interpolating the missing points in acquired GPS data. A part of acquired time-series without any missing points, which was the data at the top of one of the towers in the vertical z -direction, was taken for the verification, and some missing points; the cases of one to five missing points, were given. The least-squares interpolation was

then applied to examine the accuracy in each case. Notice that, when the number of missing data points was one or two, the difference between the interpolated and original values became less than 3 mm, which was much smaller than the accuracy of the GPS system. Figure 4 overlays the plot of the interpolated time-series and the original one in the cases of three, four, and five missing points. The residuals at the missing points are summarized in Table 1. It can be seen that the accuracies of interpolated values get lower as the number of missing points increase. In the case of five missing data points, some of the absolute residuals between the interpolated and original time-series are more than 10 mm, which is the 50 % of the measurement

Table 1 Difference between the measured values and the estimated value (unit: mm)

Sample #	3 missing	4 missing	5 missing
4	+1.6	-1.4	-4.5
5	-3.4	-7.8	-13.4
6	-4.5	-9.7	-17.5
7	-	-11.0	-19.8
8	-	-	-11.3

accuracy of installed GPS system in the vertical direction. From the results of the same verification using several time-histories, it was decided that the three missing points or less were appropriately interpolated by this least-squares based method in the target GPS data. In addition, it was recognized that the polynomial with the order $m = 3$ using three previous and two posterior data points $n = 5$ was generally able to obtain accuracies at the interpolated data points, at least better than the measurement accuracy of the GPS system. We thus applied the automatic interpolation process to many missing parts, which were with three missing points or less, in whole acquired GPS data as the pre-processing procedure for the next time-series analysis.

3 Observations of time-series GPS and temperature data and global deformation modes

The GPS time-series data used in the time-series analysis for verification here were the pre-processed data acquired from February 15th to May 15th, 2013. In Fig. 3, not only

the GPS time-series data in (a)–(c), but also the air temperature data in the same period of observation acquired by using a thermometer placed on the center span is also shown in (d); the mean value of each 1-week data is also indicated by a red line in each figure. In the case here: the displacement data from the center span, the range of displacement around the mean in the z -direction in (c), which is approximately ± 0.17 m, are much larger than those in the x - and y -directions in (a) and (b), which are both around ± 0.04 m. Compared to the time-series of the air temperature in (d), the same periodic behavior, which is almost 144 data points; i.e., 24 h, can be observed especially in the z -direction. It could be seen that the daily air temperature changes influenced the global bridge deflection. Therefore, it was considered that the analysis of the correlations between the GPS data and the air temperature could realize the understanding of the global deformations of the target bridge under the temperature changes.

The correlation coefficient analysis was then conducted. The correlation coefficient between two variables X and Y is their covariance normalized by their standard deviations, as a following function:

$$r_{X,Y} = \frac{\text{cov}(X, Y)}{\sigma_X \sigma_Y} = \frac{E[(X - \mu_X)(Y - \mu_Y)]}{\sigma_X \sigma_Y} \tag{4}$$

where μ_X and μ_Y are the mean values; σ_X and σ_Y are the standard deviations of X and Y , respectively, and $E[.]$ is the expected value operator. Four GPS locations were selected to be analyzed: the top of the north tower: #A, the top of the south tower: #D, the middle of the center span girder: #B, and the quarter of the center span girder: #C, as indicated in Fig. 2; these locations are the typical positions to

Fig. 4 Application of least-square approximation to missing data

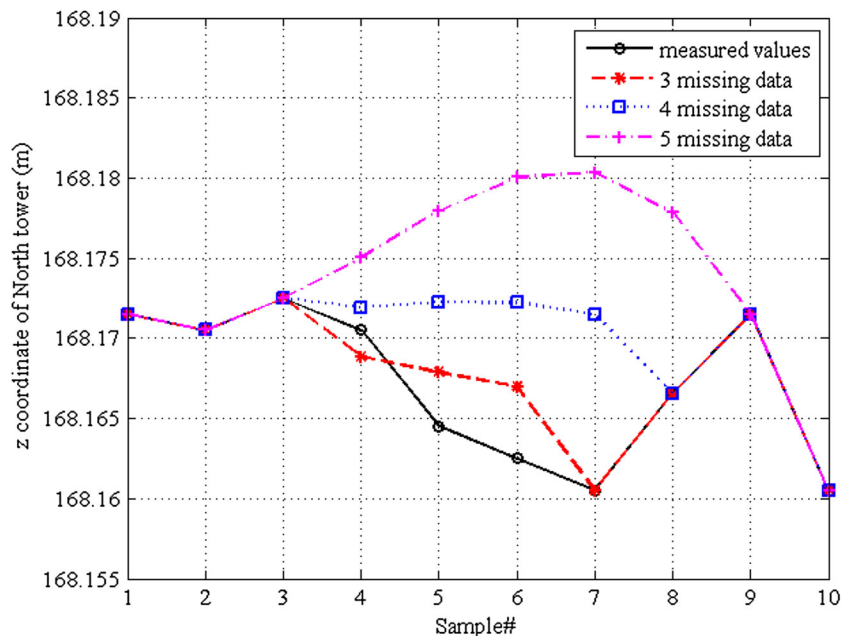


Table 2 Correlation coefficients between the GPS data and the air temperature data

Data	Temp.	North tower #A			Center span #B			Quarter span #C			South tower #D		
		x	y	z	x	y	z	x	y	z	x	y	z
North tower #A													
x	0.46	1	0.07	-0.02	0.54	0.52	-0.67	0.32	0.22	-0.56	-0.51	-0.05	0.10
y	-0.42		1	-0.36	-0.08	0.65	0.29	-0.42	0.71	0.30	-0.01	0.89	-0.33
z	0.41			1	0.05	-0.05	-0.18	0.35	-0.09	-0.13	-0.16	-0.26	0.81
Center span #B													
x	0.14				1	-0.02	-0.15	0.49	-0.09	-0.14	0.24	-0.13	0.08
y	0.06					1	-0.28	-0.17	0.80	-0.21	-0.50	0.67	-0.10
z	-0.91						1	-0.57	-0.03	0.93	0.77	0.36	-0.31
Quarter span #C													
x	0.69							1	-0.29	-0.58	-0.15	-0.49	0.48
y	-0.11								1	-0.00	-0.27	0.75	-0.17
z	-0.87									1	0.68	0.36	-0.25
South tower #D													
x	-0.61										1	0.01	-0.22
y	-0.49											1	-0.37
z	0.56												1

verify the behaviors of cable-stayed bridges. We then calculated the correlation coefficients between the air temperature and each of the GPS time-series data with all directions at location #A–D, and those between two of the GPS data as summarized in Table 2.

Firstly, when studying the correlation coefficients between the temperature and each of the GPS data at the two tower points (#A and #D), the positive and negative

correlations are recognized only in the *x*-direction, respectively. This indicates that the towers deform on the inward side when the air temperature increases; therefore, the correlation coefficients in the *y*- and *z*-directions show the negative and positive values respectively in both two towers. The influences of the air temperature on the deformations of two towers are considered to be the same because those absolute values show almost the same in all directions; from 0.4 to 0.6. On the other hand, when studying the correlation coefficients between the temperature and the GPS data from the girder points (#B and #C), it was firstly recognized that the values in the *z*-direction were much closer to -1; i.e., the negative correlation, both in #B and #C. This clearly indicates that the girder shows the global deflections as the air temperature increases. Moreover, the other correlation coefficients in the *x*- and *y*-directions show low correlations except the

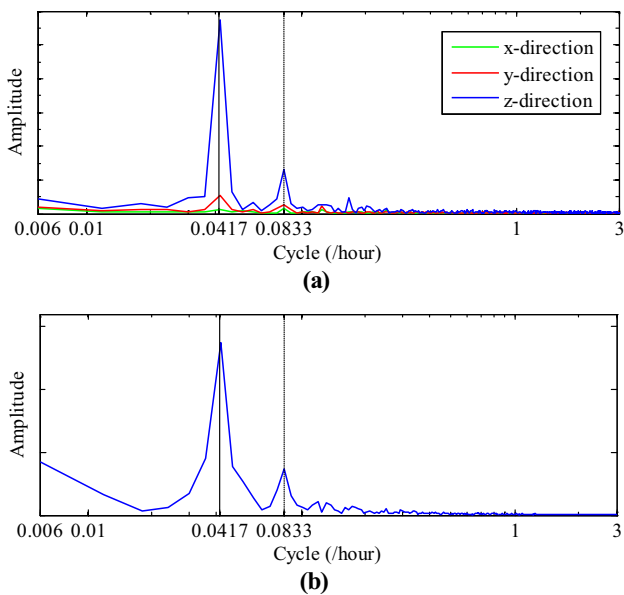


Fig. 5 Comparison of the spectra of the GPS data and the temperature data. **a** GPS data at the center span. **b** Air-temperature data

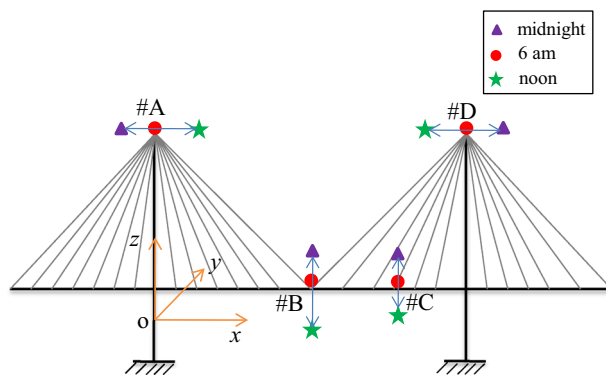


Fig. 6 In-plane global deformation modes due to the day-cycle periodic temperature change

one in the x -direction at the quarter point of the girder (#C). This can be explained that the target cable-stayed bridge was almost symmetric; therefore, the displacement in the x -direction; i.e., the longitudinal direction, did not occur especially at the center span (#B). The high negative correlation at the quarter span (#C) in the x -direction was then observed because the location there was the non-symmetric position of the girder. Lastly, the correlation coefficients in the y -direction at both #B and #C are very small; therefore, it can be said that the in-plane deformation (the x - z coordinate) of the cable-stayed bridge is dominated in the global deformation of the girder.

In addition, the frequency (/h) spectra of the GPS data and the air temperature data were derived to compare the dominated frequencies of those time-series. Figure 5a, b are obtained spectra; (a) is from the 1-week GPS data at the center span, which is exactly the time-series presented in Fig. 3a–c, and Fig. 5b is from the temperature data in Fig. 3d. Here, the dominated frequency (/h) components in the target time-series can be examined within the range from 0.00595/h (=1 week, 7 days) to 3/h (20 min). It can be seen that the same two frequencies show high amplitudes; the highest one is 0.0417/h (= 24 h) and the other is 0.0833/h (= 12 h) in two spectra: the GPS data in the z -direction and the air temperature data. Notice that the GPS data in the z -direction at the center span show the highest absolute correlation coefficient. This indicates that the GPS data show high correlation with the air temperature, are mostly dominated by the 1-day periodic behavior, which is the 24 h-cycle; the highest and lowest temperatures are thus observed at the noon and at the midnight, respectively.

On the basis of those results, the global deformation modes due to the periodic temperature changes could be identified as shown in Fig. 6. Here, the x - and z -displacements at the midnight and the noon calculated by differencing the x - and z -coordinates from those at 6 am in a certain day were plotted in the four considering points: #A–D. Notice that the same symbols show the displacements at the same time of observation. It can be understood that the global deformation mode due to the increase of air temperature is configured by the inward deformations of the two towers and the downward vertical deflection of the girder, and the reverse occurs when the temperature decreases. In seeing the correlation coefficients between two of GPS data presented in Table 2, high absolute correlations can be observed not only between the z -directions at the two points of the girder, but also between two of all directions at the two towers, and between the z -direction at the girder and the x -direction at each of the towers.

From those results, the deformation due the air temperature changes was recognized. It was then concluded that the displacements of the two towers and the girder in the deformation due to the 1-day periodic temperature

change are highly correlated; therefore, the statistical pattern recognition of those global deformation was expected to be applicable for assessing the condition of the structure globally using the GPS data.

4 Application of the time-series analysis to GPS data for structural condition assessments

On the basis of the considerations in the previous chapter, we then verified the applicability of the time-series analysis to the feature extraction for the structural condition assessment that statistically investigated the pattern of the global deformations. Here, the autoregressive integrated moving average (ARIMA) model was adopted because the global deformation was understood to be dominated by the 1-day periodic behavior. From the results in the previous chapter, we then picked up some data to be analyzed; they were the data in all of three directions at the top of two towers, the data in the z -direction at the center span of the girder, and the data in the x - and z -directions at the quarter span, all of which showed the high correlation coefficients with the air temperature data.

4.1 Description of ARIMA model

The ARIMA model is a statistical models to describe non-stationary time-series [14]. The model is generally described as ARIMA(p, d, q), where p, d and q are the orders of the model, and it is defined as:

$$(1 - \phi_1 B - \phi_2 B^2 - \dots - \phi_p B^p)(1 - B)^d y_t = c + (1 - \psi_1 B - \psi_2 B^2 - \dots - \psi_q B^q) \varepsilon_t, \tag{5}$$

where y_t is the t -th component of the target time-series vector y , and ε_t is the white noise error term. ε_i ($i = 1 - p$) and ε_j ($j = 1 - q$) are coefficients of the autoregressive term and the moving average term, respectively, and B is the lag-operator, which is defined as:

$$B^k y_t = y_{t-k}; \tag{6}$$

therefore, $(1 - B)^d$ in Eq. (5) indicates the d -th order difference of the original time-series. By taking the difference, the trend in the time-series can be removed, and the non-stationary process can be transferred to the stationary process.

Figure 7a is a part of the one of the GPS time-series data, which is the 1-week extracted data (from Feb 15th to 22nd, 2013) in the z -direction acquired at the center span of the girder, and (b) is its autocorrelation function (ACF). The apparent 144 points; equal to 1-day, which have the periodic behaviors with a slow damping is clearly observed; it can thus be said that the data is non-stationary and influenced by the 1-day periodic temperature change.

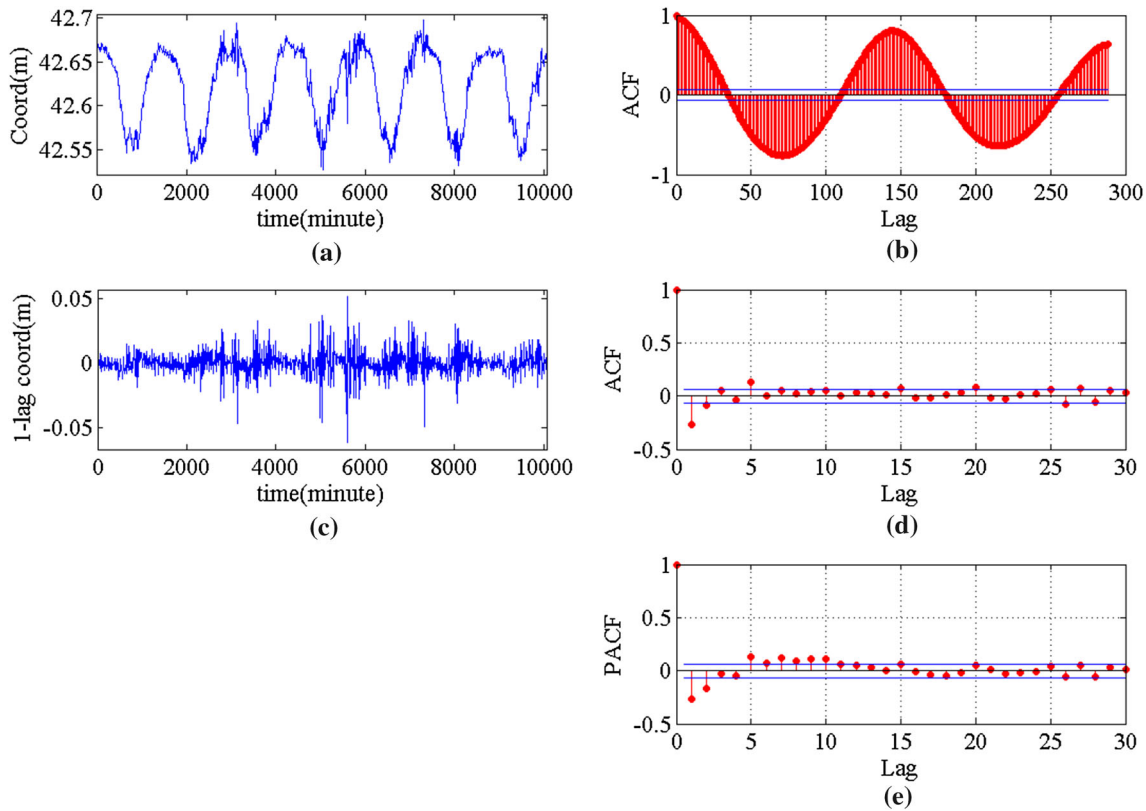


Fig. 7 ACF and PACF of GPS time-series data and its differentiated time-series. **a** GPS time-series data, **b** ACF of GPS time-series data, **c** taking differentiated, **d** ACF of differentiated series, **e** PACF of differentiated series

By taking the first order difference ($d = 1$) as shown in Fig. 7c, the ACF then dropped quickly to within the 95 % confidential interval indicated by blue lines, as shown in Fig. 7d. To check whether the differenced time-series was stationary or not, the Augmented Dickey Fuller (ADF) test [14] was also conducted. The null hypothesis here was: “the first order differentiated data was non-stationary.” The statistical possibility p value was then calculated at 0.001 that was smaller than the 5 % significant level, and the absolute test statistic value was 41.51 that was much larger than the absolute critical value 3.41. Therefore, the null hypothesis here was rejected; it indicated that the original time-series was transferred to stationary by taking the first order difference.

Table 3 BIC results for the definition of ARIMA model order

	MA(q)			
	1	2	3	4
AR(p)				
1	-7847	-7846	-7839	-7824
2	-7844	-7832	-7824	-7832
3	-7838	-7824	-7826	-7828
4	-7833	-7826	-7829	-7823

When the time-series became stationary by taking the difference, the orders of AR process p and MA process q in ARIMA(p, d, q) were determined by the partial autocorrelation function (PACF) and the ACF [14]. Those for the differentiated time-series are shown in Fig. 7d, e. It can be seen that the values are almost contained within the 95 % confidential interval at lag = 2 in ACF and lag = 3 in PACF; therefore, $q = 1$ and $p = 2$ can be accepted for the MA and AR orders, respectively. However, the values of PACF are not completely decayed inside the confidential interval after the identified lag.

To determine those orders p and q clearly, the Bayesian information criterion (BIC) method was additionally examined. The BIC is one of criteria for the model selection among a finite set of models. It is based on the likelihood function and closely related to the Akaike information criterion (AIC) [14, 15]. The formula of BIC is:

$$BIC = -2 \ln \hat{L} + k \ln(N), \tag{7}$$

where \hat{L} is the maximized value of the likelihood function of the model, N is the length of data, k is the number of free parameters. The verifications were then conducted by calculating the BICs to the ARIMA models for several GPS time-series data using the MATLAB function “aicbic”. Here, the $\ln \hat{L}$ is the optimized log-likelihood function

obtained in the estimation of each ARIMA model. One of the results, which is obtained from a 1-week GPS data acquired at the center span, is shown in Table 3. The row the table corresponds to the AR order p from 1 to 4, and the column is the MA degree q also from 1 to 4. Notice that the order d of ARIMA(p, d, q) is all $d = 1$ on the basis of the results discussed for Fig. 7. It can be seen that the smallest BIC value is calculated in $(p, q) = (1,1)$; the orders p, d , and q were thus determined to ARIMA(1, 1, 1) that is the appropriate model to apply for GPS data in this study.

4.2 Discussions for estimated AR-MA coefficients distributions

The coefficients of the ARIMA model estimated for the GPS data that consist of 1-day periodic behaviors were considered to be applicable as the feature to indicate the global deformation modes of the target Can Tho bridge. We verified this by applying the ARIMA model estimation to the data from February 15th to May 15th, 2013. Notice that the data to be analyzed were the data in all of three directions at the top of two towers (#A and #D), the data in the z -direction at the center span of the girder (#B), and the data in the x - and z -directions at the quarter span (#C), as mentioned in the previous chapter. The GPS data were taken to divide into day by day, and ARIMA(1,1,1) model was estimated to each of 1-day time-series. Figure 8 shows one of the results that is from one of 1-day GPS time-series in the z -direction at the center span. The time-series from the estimated ARIMA model and the original one are overlaid in Fig. 8a and b is the standardized distribution of the residual errors with the standardized normal distribution. Here, the Ljung-Box Q-test (LBQ-test) [14] was also conducted to check whether the residual error distribution showed the white noise process with the normal distribution. The null hypothesis here was; “the residual was the white noise.” In

the results, the statistical possibility p values at lags (5, 10, 15) were (0.0624, 0.1668, 0.3410) that were all larger than the 5 % significant level, and the test statistic values were calculated at (7.3199, 11.6650, 14.4788), which were smaller than the critical values at 5 % significant level (7.8147, 15.5073, 22.3620). It means that the null hypothesis was not rejected. The residuals were thus identified as the white noise process. We also checked those performances in the estimations for other 1-day time-series and confirmed that the estimations were conducted with almost the same and appropriate accuracies.

Figure 9 shows the plots of the estimated AR and MA coefficients from every 1-day time-series data for all considered time-series GPS data. In all figures, the plots are categorized by different markers depending on the data for each month. Before the discussions here, it should be noticed that any significant structural condition changes had not been reported during this period in the Can Tho bridge. Because the regressions are recognized in all plots, the R -square values for the linear regressions are also indicated. Relatively high R -square values are then shown in the plots from the GPS data in the z -direction at both the center and quarter spans (#B and #C), those in the x -direction at the top of two towers (#A and #D), and those in all directions at the top of South tower (#D). In those data, the correlation coefficients with the temperature also showed high values, as mentioned in Table 2. Therefore, those regressions are considered to indicate the pattern of the global deformation due to the 1-day periodic temperature change statistically. Any outlier detection procedure should be adopted for the statistical structural condition diagnosis. However, it can be said that those regressions in the AR-MA coefficients from the ARIMA model can be used as the base distributions there. It was then concluded that the global deformations due to the 1-day periodic temperature change could be used for the global structural condition assessment.

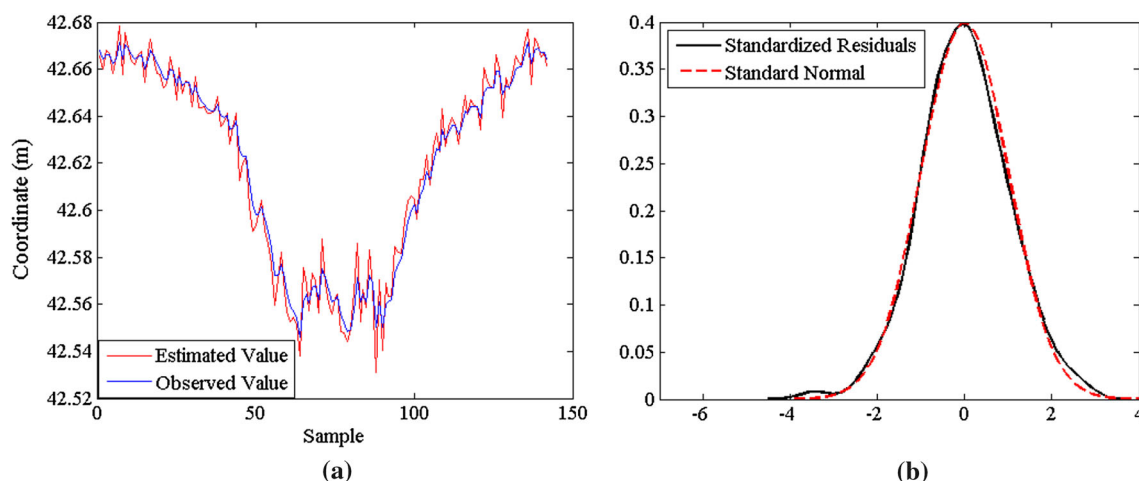


Fig. 8 Estimation of ARIMA model. a Overlay of estimated and measured time-series. b Distribution of residual error

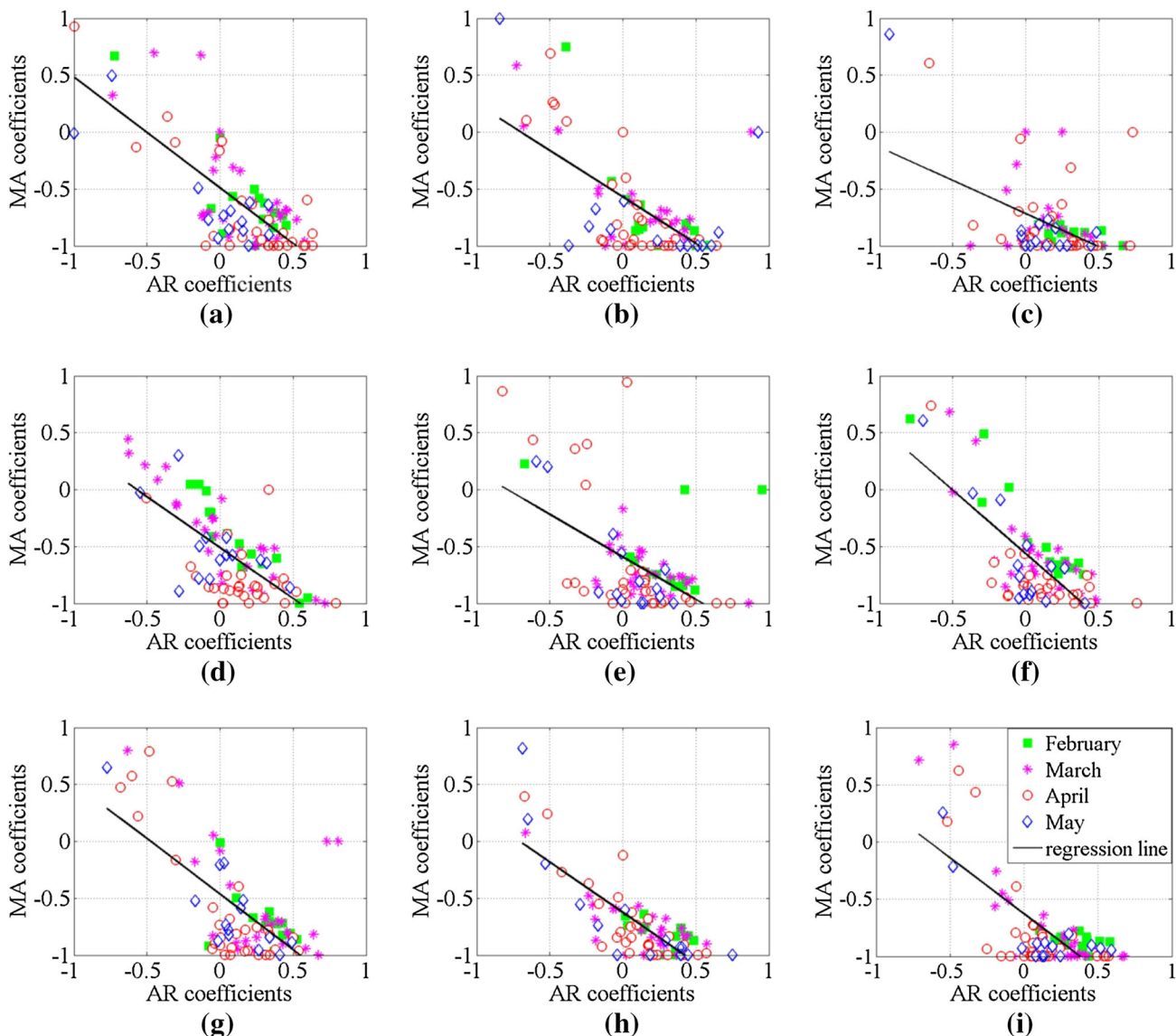


Fig. 9 AR-MA coefficients distributions. **a** *x*-direction at #A ($R^2 = 0.578$) **b** *y*-direction at #A. ($R^2 = 0.479$) **c** *z*-direction at #A. ($R^2 = 0.221$). **d** *z*-direction at #B. ($R^2 = 0.486$). **e** *x*-direction at #C ($R^2 = 0.281$). **f** *z*-direction at #C ($R^2 = 0.557$). **g** *x*-direction at #D ($R^2 = 0.505$). **h** *y*-direction at #D ($R^2 = 0.641$). **i** *z*-direction at #D ($R^2 = 0.519$)

5 Conclusions

This paper studies the analysis of GPS time-series data acquired in a long-span cable-stayed bridge, and considers the applicability of time-series analysis that is the aim of identifying global deformation patterns for the structural condition assessment. The results can be summarized as below:

- The correlation coefficients analysis was conducted using the pre-processed GPS data with the interpolation

of missing data. The data in the significant directions at the two towers and the girder showed high correlation with the air temperature data.

- It was also shown that the GPS data has high correlation with the temperature dominated by 1-day periodic behaviors. In addition, most of the GPS data that relate to the global deformation were also highly correlated each other. The global deformation mode due to the 1-day periodic temperature change could then be clarified, and the significant displacements of the two towers and the girder were also shown.

- To extract the features that can indicate the pattern of the global deformation, the applicability of estimating ARIMA model was verified. The GPS time-series data was recognized as the non-stationary data, and it could be transferred to the stationary process by taking the first difference.
- When apply the ARIMA(1, 1, 1), that its orders were determined by ACF, PACF, and BIC, for the three-months GPS data, the plots of estimate AR-MA coefficients showed the regressions especially in the data showed high correlation coefficients with the temperature data; i.e., the time-series that were dominated by the global deformation mode.

From the last results, those AR-MA coefficients were expected to be used as the features to assess the structural conditions. When those plots are treated as the baseline distributions, the changes in the global deformation are considered to be detected by adopting any multivariate outlier detection algorithm. This is actually our next work to realize a statistical structural condition diagnosis procedure. However, in this study, the global deformation due to the 1-day periodic temperature change was clarified, and it was also shown that those global deformations could be used for the global structural condition assessment by applying the ARIMA model.

References

1. Kaloop MR, Li H (2009) Monitoring of bridge deformation using GPS technique. *KSCE J Civil Eng* 13(6):423–431
2. Kaloop MR, Li H (2011) Sensitivity and analysis GPS signals based bridge damage using GPS observations and wavelet transform. *Measurement* 44(5):927–937
3. Celebi M (2000) GPS in dynamic monitoring of long-period structures. *Soil Dyn Earthq Eng* 20(5):477–483
4. Cheng P, John W, Zheng W (2002) Large structure health dynamic monitoring using GPS technology. In: FIG XXII International Congress, Washington DC
5. Fujino Y, Murata M, Okano S, Takeguchi M (2000) Monitoring system of the Akashi Kaikyo Bridge and displacement measurement using GPS. In: SPIE's 5th Annual International Symposium on Nondestructive Evaluation and Health Monitoring of Aging Infrastructure. International Society for Optics and Photonics, pp 229–236
6. Sohn H, Dzwonczyk M, Straser EG, Kiremidjian AS, Law KH, Meng T (1999) An experimental study of temperature effect on modal parameters of the Alamosa Canyon bridge. *Earthq Eng Struct Dyn* 28(8):879–897
7. Cornwell P, Farrar CR, Doebling SW, Sohn H (1999) Environmental variability of modal properties. *Exp Tech* 23(6):45–48
8. Farrar CR, Cornwell P, Doebling SW, Prime MB (2000). Structural health monitoring studies of the Alamosa Canyon and I-40 bridges. Los Alamos National Laboratory, LA-13635-MS
9. Omenzetter P, Brownjohn JMW (2005) A seasonal ARIMAX time series model for strain-temperature relationship in an instrumented bridge. *Proceedings of the 5th International Workshop on Structural Health Monitoring*, pp 299–306
10. Omenzetter P, Brownjohn JMW (2006) Application of time series analysis for bridge monitoring. *Smart Mater Struct* 15(1):129–138
11. Sohn H, Czarnecki JA, Farrar CR (2000) Structural health monitoring using statistical process control. *J Struct Eng* 126(11):1356–1363
12. Pigott TD (2001) A review of methods for missing data. *Educ Res Eval* 7(4):353–383
13. Gerald CF, Wheatley PO (2004) *Applied numerical analysis*. 7th edn, chapter 3, pp 203–207
14. Shumway RH, Stoffer DS (2010) *Time series analysis and its applications: with R examples*. Springer
15. Hirose K, Kawano S, Konishi S, Ichikawa M (2011) Bayesian information criterion and selection of the number of factors in factor analysis models. *J Data Sci* 9(2):243–259